Clim. Past Discuss., 4, 981–1019, 2008
www.clim-past-discuss.net/4/981/2008/

Climate of the Past Discussions

Climate of the Past Discussions is the access reviewed discussion forum of *Climate of the Past*

Modelling Maastrichtian climate: investigating the role of geography, atmospheric CO_2 and vegetation

S. J. Hunter[1,3], P. J. Valdes[2], A. M. Haywood[3], and P. J. Markwick[4]

[1]British Antarctic Survey, NERC, High Cross, Madingley Road, Cambridge, CB3 OET, UK
[2]BRIDGE, School of Geographical Sciences, University Road, Bristol, BS8 1SS, UK
[3]School of Earth and Environment, University of Leeds, Leeds, LS2 9JT, UK
[4]GETECH, Kitson House, Elmete Hall, Elmete Lane, Leeds, LS8 2LJ, UK

Received: 25 July 2008 – Accepted: 29 July 2008 – Published: 25 August 2008

Correspondence to: S. J. Hunter (shunter@bas.ac.uk)

Published by Copernicus Publications on behalf of the European Geosciences Union.

Abstract

In this paper we describe the results from an ensemble of palaeoclimate simulations of the Maastrichtian using the fully-coupled dynamic ocean-atmosphere General Circulation Model, HadCM3L. Using appropriate Maastrichtian boundary conditions, we investigate the sensitivity of the predicted palaeoclimate to changing atmospheric CO_2 levels and modelled vegetation treatment. In addition, we explore the climatic response to the changed geography using a comparison with a pre-industrial experiment. We describe our results alongside the findings of previous modelling studies in particular with consideration to concepts of climate equability. Our findings demonstrate increased global temperatures compared with the pre-industrial experiment, with a 5.9°C increase in temperatures associated with the change to 1×CO_2 Maastrichtian conditions and a further 3.9°C warming associated with a quadrupling of atmospheric CO_2 levels. Compared to the pre-industrial we find a latitudinal temperature profile that is reduced in gradient and shifted to higher temperatures. Our control 4×CO_2 Maastrichtian experiment exceeds the pre-industrial by 6.5–8.6°C, 7.4–11.2°C, and 10.1–32.4°C in the equatorial, mid and high latitudes respectively. We also find a general pattern of increased thermal seasonality in the high latitudes. In terms of global mean annual temperatures we find a range of 18.1–23.6°C for our 1–6×atmospheric CO_2 envelope. Other than in the northern high latitudes we find satisfactory levels of agreement between the ensemble temperature envelope and estimates from palaeotemperature proxies. The inclusion of a dynamic vegetation model (TRIFFID) leads to a further increase in the thermal seasonality at high latitudes, warming in the mid to high latitudes and increased precipitation in the low and mid latitudes.

1 Introduction

Through the use of geological climate proxies, the Cretaceous period has generally been characterised as a world with elevated global temperatures and increased equa-

bility in the climate system (Frakes, 1979; Barron, 1983; Hallam, 1985). Here, climate equability is defined as reduced climatic extremes in terms of seasonal cycle and a reduced equator-to-pole temperature gradient generated by warmer polar temperatures (Sloan and Barron, 1990; Valdes et al., 1996).

The Maastrichtian stage, lasting from 71.3 to 65.0 Ma, immediately precedes the terminal mass-extinction event at the Cretaceous-Tertiary (K/T) boundary. A significant coverage of geological evidence also suggests that the Maastrichtian was a time of great variability in the climate and ocean systems (Wolfe and Upchurch, 1987; Barrera, 1994; Li and Keller, 1998, 1999; Francis and Poole, 2002; Gallagher et al., 2008).

The Maastrichtian world can be split into two distinct hemispheres, one dominated by the deep oceanic basin of the Pacific and the other consisting of the well-dispersed continents originating from the Laurasian and Gondwanan continental blocks. An extensive east-west subtropical ocean, the Tethys, joins the North Atlantic and Caribbean with the proto Indian Ocean in the west. The Atlantic Ocean is much narrower than in the present day. The continents, particular of the northern hemisphere, are partially covered with extensive, although shallow, epicontinental seas. The Western Interior Seaway (WIS) and the Turgai Strait (via the Western Siberian Sea) provide shallow seaway linkages into the Arctic Ocean. In the southern hemisphere, India is an island continent, adrift in the Southern Ocean. South America (Case et al., 2000; Lawver et al., 1992) and Australia (Exon et al., 2001; Brown et al., 2006) are connected to Antarctica by island chains and shallow seaways. A reconstruction of the palaeogeography, as developed within Markwick and Valdes (2004) can be seen within Fig. 1.

Studies using fossil leaf stomatal abundance and palaeosol proxies suggest that the Maastrichtian atmospheric CO_2 level ranged between ~1 and 6×pre-industrial levels (Cojan et al., 2000; Ghosh et al., 2001; Beerling et al., 2002; Nordt et al., 2002, 2003).

The geological evidence in support of elevated temperatures is extensive. This includes sea-surface mean annual temperatures (hereafter referred to as SST) of 28–30°C in the tropical Indian Ocean (Pearson et al., 2001) and high summer temperatures in the arctic ocean of 15°C (Jenkyns et al., 2004). Bathyal temperatures have

been predicted as high as 12–9°C at 1200–1500 m palaeodepth (Huber et al., 2002) and 14–10°C at 1000–3000 m palaeodepth (Barrera et al., 1987). Terrestrial data is also well represented, with fossil floras and faunas indicative of warmer climates being found at higher-than-present latitudes. Using oxygen isotope analysis of reptilian tooth enamel, Amiot et al. (2004) found a shallower-than-present-day latitudinal temperature gradient from 30°C to the pole. This is supported on the Antarctic Peninsula, where physiognomic analysis of fossil angiosperm woods suggest a mean annual temperature (hereafter referred to as MAT) of between ~7–15°C at 59–62° S (Francis and Poole (2002, and references therein) and Poole et al. (2005)). In addition, a MAT of between 12–15°C was found on the South Island, New Zealand, a palaeolatitude of 60° S (Kennedy et al., 2002). In the northern hemisphere, an estimated MAT of 2–8°C was derived using similar methods on the North Slope of Alaska, palaeolatitude 80–85° N (Parrish and Spicer, 1988).

Here we present an analysis of an ensemble of simulations of Maastrichtian climates using the HadCM3L coupled atmosphere-ocean GCM. We develop upon previous modelling studies by presenting an ensemble of experiments to understand the response of the predicted climate to geologically supported variations in atmospheric CO_2 and changes in the modelled vegetation treatment.

2 Results from previous cretaceous climate modelling studies

Many early climate-modelling studies of the Cretaceous focussed upon the mid-Cretaceous period as this warm period was well represented within the geological record. Mostly using atmosphere-only GCMs, these studies investigated the hypothesis of climate equability; how an ice-free world could be maintained; and the role of atmospheric CO_2 (Barron et al., 1981; Barron and Washington, 1982; Barron, 1983; Barron and Washington, 1985; Sloan and Barron, 1990). To address these hypotheses, changes in the geography, atmospheric composition, meridional energy transport, and high-latitude surface albedo were investigated. Although the mid Cretaceous was found to

be significantly warmer than present day, the models found it difficult to reproduce a mid-Cretaceous climate that was fully compatible with the geological record. In particular, problems existed in replicating year-round polar warmth (Barron and Washington, 1985), latitudinal temperature gradients (Barron, 1983) and continental interior temperatures (Barron and Washington, 1985; Sloan and Barron, 1990).

Barron and Washington (1985) investigated the climatic effect of mid-Cretaceous geography. They found that the land-sea distribution could account for a substantial amount of the Cretaceous warmth. Barron and Washington (1985) also considered how elevated atmospheric CO_2 levels could warm the polar-regions finding this was also accompanied by unreasonably large increase in low-latitude warmth. They found that a quadrupling of atmospheric CO_2 lead to an increase in a global mean increase in temperature of 3.6°C. These early simulations relied upon atmospheric general circulation models that did not simulate a seasonal cycle. The inadequacies of these models were thought to account for the discrepancies between the simulated climates and the proxy record, as well as providing unrealistic climate sensitivities. Using a simplified energy balance model, Crowley et al. (1986) considered the influence of the land-sea distribution on driving seasonality. They found that since the late Cretaceous, the geographical driven change in seasonality, expressed through peak summer temperatures, was comparable in magnitude to the temperature change due to a doubling of CO_2. Barron et al. (1993) revisited the role of geography using a full seasonal-cycle atmospheric GCM coupled to a slab ocean model. Regional temperature changes did occur due to re-arrangement of land and ocean, but they found geography to be less of a driver of global warmth than previously thought. In this model, Barron et al. (1993) found that a quadrupling of CO_2 lead to an increase in global averaged temperature of 5.5°C – a greater sensitivity than previously predicted. In addition, they suggested the inclusion of a more detailed and complete oceanic circulation models would help resolve the distribution of Cretaceous warmth. Bush and Philander (1997), using a GCM with an idealised Late Campanian/Maastrichtian palaeotopography and bathymetry, found a 4°C sensitivity in global temperatures from a quadrupling of atmospheric CO_2,

with most warming occurring at the high-latitudes. The northern and southern high-latitudes warmed by 18–20 and 30–35°C respectively, the equatorial region by ∼5°C and the mid latitudes the least at ∼2–3°C warming.

Using a coupled atmosphere-ocean model, Bush and Philander (1997) focussed upon the late Cretaceous seasonal cycle. In addition to possessing flat continents, the model lacked shallow epicontinental seas and had oceans defined with fixed 5700 m bathymetry. The seasonal cycle was reduced, thought mostly to originate from the lack of both permanent ice on the poles and snowfall within continental interiors. Combining the reduced seasonal cycle with the increased MAT led them to conclude a lack of year-round snow or ice at high latitudes. Regarding the climate as a whole, they concluded that the latitudinal trend of surface temperatures is indicative of an equable climate, despite many similarities in profile with the modern-day.

The need to consider the role of vegetation in palaeoclimatic modelling studies is well documented (Cosgrove et al., 2002, and references therein). Early GCM sensitivity experiments of the Cretaceous (such as Barron and Washington (1985); Barron et al. (1993)) relied upon primitive land surface schemes; often consisting of blanket coverage of savannah or shrub-land. It became apparent that such a simplistic treatment could lead to errors in the simulated temperature and precipitation fields (Cosgrove et al., 2002). Otto-Bliesner and Upchurch (1997) considered how the role of vegetation could explain discrepancies between modelled and geological evidence, in the continental interiors and high latitude temperatures. Earlier models, such as those of Barron and Washington (1982); Sloan and Barron (1990), commonly predicted continental interiors that were colder than predicted by the geological proxies. Using a late Maastrichtian palaeogeography and 2×pre-industrial CO_2 levels, Otto-Bliesner and Upchurch (1997) used a standard bare-earth model alongside one with prescribed vegetation based upon a geological best estimate. It was found that the inclusion of high and mid latitude forest vegetation increased the global mean temperature by 2.3°C, the tropics by 1.5°C and the northern and southern high latitudes by 4.1 and 3.4°C respectively. Most of this heating occurred through the summer months.

In addition, the vegetation reduced the areal extent and duration of sea-ice. Upchurch et al. (1998) documented a more detailed and extensive comparison of different land-surface schemes, which included bare soil and evergreen tree blanket coverage, as well as geologically derived vegetation schemes. High latitude forest vegetation introduced feedbacks into the climate system between surface energy exchange, surface temperatures and snow and ice. As well as supporting high latitude warmth at times during the Maastrichtian the work demonstrated the importance of considering or including realistic vegetation into a model. DeConto et al. (1999) used the Vegetation Ecology model (EVE) and the GENESIS GCM to investigate principally the climate of Campanian continental interiors. They found that with the inclusion of dynamic vegetation, they could successfully reproduce the low latitudinal temperature gradients and continental interior winter-warmth supported by geological evidence. In support of Upchurch et al. (1998), DeConto et al. (1999) found that the presence of high latitude forests played an important role in supporting polar warmth.

The Cretaceous Ocean system has also been the focus of several papers. Early studies such as those of Barron and Peterson (1989, 1990); Bush and Philander (1997) considered the circulation through the Tethys in particular with regards to circum-global currents. These early simulations, using relatively low-resolution palaeogeographies, failed to reproduce the general westward flow suggested by palaeo-biogeographical and laboratory studies (Barron and Peterson, 1989). Using a high-resolution palaeogeography capable of resolving the narrow seaway currents, Bush (1997) found a westward flowing current in agreement with the evidence, and suggested that previous studies had failed to replicate this flow due to the limited spatial resolution and the specified continental configuration used within the models. Hay and DeConto (1999) in a study of poleward energy transportation considered the structure and circulation of the Campanian Ocean on a global scale. They found greater regional salinity differences than the present-day which led them to suggest a greater role of salinity in driving surface ocean circulation than at present. With the implementation of increasingly powerful computers, later studies began considering the circulation of the deeper ocean. Otto-

Bliesner et al. (2002) investigated the sources of warm ocean bottom waters in the Campanian ocean. They found a thermohaline circulation significantly different from the present day, with each hemisphere consisting of a deep (5 km) overturning cell extending further poleward than the present North Atlantic cell.

3 Methods

3.1 The GCM: the UK met office unified model

An in-depth description of the Unified Model used in this study can be found within Gordon et al. (2000). For convenience a brief description follows. The model was developed at the Hadley Centre for Climate Prediction and Research, part of the UK Meteorological Office, and is one of the first to be developed without the requirement for flux-adjustments (Gregory and Mitchell, 1997). The GCM consists of dynamically and thermodynamically coupled atmosphere, ocean and sea-ice components (Gordon et al., 2000) The particular version of the Unified Model used within this study is HadCM3L, differing from HadCM3 in the implementation of a lower resolution ocean model. The horizontal resolution of the atmosphere and ocean models is 2.5° in latitude by 3.75° in longitude, approximating a spectral resolution of T42. This leads to a spatial resolution at the equator of 278 by 417 km in north-south and east-west directions respectively. In the vertical direction there are 19 levels in the atmosphere and 20 in the ocean. The treatment of atmospheric physics is identical to that used within HadCM3, with a time step of 30 min and coupling to the ocean component made once every simulated day. Other than modifications that take into account the reduced spatial resolution Gent and McWilliams (1990) the ocean physics treatment is again identical to that found within HadCM3L (Gordon et al., 2000).

HadCM3 (identical to HadCM3L except for a high resolution ocean) had been used within the IPCC 4th assessment report and the PMIP2 study (the second Palaeoclimate Modelling Intercomparison Project, Gladstone et al., 2005). In addition, HadCM3 and

its model components have been used successfully in a number of pre-Quaternary modelling studies (Haywood and Valdes, 2004; Lunt et al., 2007).

3.2 The dynamic vegetation model: TRIFFID (Top-down Representation of Interactive Foliage and Flora Including dynamics)

As part of this study we have employed the TRIFFID vegetation model coupled to the HadCM3L GCM. The model is detailed within Cox (2001); Cox et al. (2001), so only a brief introduction will be given here. Developed by the Hadley Centre, the model defines the state of the terrestrial biosphere in terms of soil carbon and the structure and coverage of five different plant functional types (broad and needle leaf trees, C3 and C4 grasses, and shrubs) within each model grid box. The distribution and characteristics of these functional types is derived using a carbon balance model in which vegetation change is driven by net carbon fluxes calculated by the MOSES 2 (Met Office Surface Exchange System) land surface scheme (Cox et al., 2001). In this way, TRIFFID attempts to treat the direct effects of CO_2 on the vegetation and the subsequent biogeophysical and carbon-cycle feedback-effects on the climate. Although TRIFFID relies upon representations of modern vegetation-coverage types, such as C3 and C4 grasses, we assume that during the Cretaceous these niche areas were represented by some ancestral analogue with similar coverage and interaction with the terrestrial biosphere. When in use, TRIFFID is run for 50 simulated years for every 5 years simulated within the GCM.

4 Experimental design

4.1 Boundary conditions

In any palaeoclimate modelling study, the important boundary conditions are the land-sea distribution, land coverage, the topography and bathymetry, atmospheric composition, the orbital configuration and the solar intensity. The Maastrichtian geography,

which incorporates the land-sea distribution, topography and bathymetry, is taken from Markwick and Valdes (2004). The GCM representation of the land-sea distribution can be seen within Fig. 2. The plate reconstruction corresponds to the early Maastrichtian at an age of 69.4 Ma according to Gradstein and Ogg (1996). Data of a Maastrichtian age (71.3–65.0 Ma) is utilised in the compilation of topography and bathymetry data points (Markwick and Valdes, 2004), the palaeogeography is therefore considered representative of a generalised Maastrichtian time slice (see Fig. 1). The relatively coarse spatial resolution of the GCM does at times impose interpretational uncertainty when we consider important subscale geographical features such as seaways and land linkages. One such example is the extent and representation of arctic seaway connections with the Tethys Ocean and Western Interior Seaway, which will be subject of a later study. These connections became more restricted during the late Maastrichtian, eventually isolating the Arctic Ocean.

Surface coverage is set to a shrub everywhere and stays fixed. We use a sensitivity experiment to investigate the affect of a more rigorous land-surface treatment, implementing the previously described TRIFFID dynamic vegetation model and the MOSES 2 land surface scheme.

We set atmospheric CO_2 levels as 1, 2, 4 and 6×pre-industrial levels (280 ppmv). Geological proxies indicative of the other important greenhouse gas components, such as methane and nitrous oxide, are unavailable and so we set these along with the remaining atmospheric components to modern-day levels. The vertical distribution of ozone is allowed to thermodynamically expand inline with the warmer troposphere.

For all the experiments the orbit is circular (zero eccentricity) with present-day obliquity (23.4°). The solar intensity is reduced by 0.5% to account for the dimmer, younger Sun (Kump et al., 1999).

4.2 Ensemble approach

An ensemble of seven GCM experiments address the sensitivity of the climate to changes in atmospheric CO_2 and land-surface treatment. These experiments are sum-

marised within Table 1. We define a Maastrichtian control experiment with four-times the pre-industrial level of atmospheric CO_2 (hereafter referred to as Maas4^{CON}. We compare this against the sensitivity experiments, considering changes in the climate system and upper-ocean. Where appropriate, we compare the GCM output against the available geological climate proxies. For completeness, a comparison against a pre-industrial experiment is carried out (hereafter referred to as PreInd).

The GCM is typically spun up for a total of 170 years and the climate variables are derived from the subsequent 30 years. Although this spin-up time is insufficient to allow equilibrium to be reached in the deep-ocean circulation, it is adequate for the upper-ocean and atmospheric diagnostics.

5 Model results

5.1 Temperature

The modelled global mean near-surface air temperatures are given in Table 1. We find a climate sensitivity for the Maastrichtian of 3.9°C for a quadrupling of CO_2, from 1 to 4×. The all-surface meridional temperature profiles are shown within Fig. 3. The Maas4^{CON} experiment exceeds PreInd by 6.5–8.6°C and 7.4–11.2°C in the equatorial and mid latitudes respectively. In the high latitudes we see a larger asymmetry in warming, the northern hemisphere exceeds PreInd by 12.2–17.5°C and the southern hemisphere by 10.1–32.4°C. These zonal values suggest a shallower latitudinal temperature gradient, which, other than at high latitudes, is not obvious in Fig. 3a. This discrepancy is due to the difference in the latitudinal distribution of landmasses between the Maastrichtian and modern-day, making direct comparison difficult. At high latitudes, the model predicts much warmer conditions, resulting from a lack of any permanent ice in the polar-regions. The pattern of latitudinal warming is similar to that predicted by Bush and Philander (1997), except in the mid-latitudes, where Bush and Philander found minimal (∼2–3°C) warming.

Comparing Maas1 against PreInd we find a 5.9°C warming. It is not possible to associate this warmth with a single driving factor, as the differences in the two experiments are numerous (geography, land-surface scheme, reduced solar constant). The inclusion of the dynamic vegetation model, TRIFFID, increases the global mean temperature at 4×CO_2 by 0.2°C, significantly less than the 2.3°C found by the 2×CO_2 Maastrichtian studies of Otto-Bliesner and Upchurch (1997). The change in the land and ocean latitudinal temperature distributions due to the implementation of TRIFFID can be seen within Fig. 3b. The heating observed at mid and high latitudes occurs mostly over land areas with ∼1.5°C and ∼1°C average warming in the northern and southern hemispheres respectively.

The spatial distribution of the Maas4^{CON} and PreInd MAT can be seen within Fig. 4. For the Maastrichtian we find the highest temperatures occur consistently in North Africa, equatorial South America, and South-Eastern Asia. The tropical 24°C isotherm expands poleward by between ∼15–30° generally greater than the 10–15° expansion found within the 4×CO_2 experiment of Bush and Philander (1997). The mean annual temperature is above freezing except beyond ∼55–70° N and ∼70–75° S for the range of CO_2 values. The coldest winter temperatures occur in the interior of Antarctica, with temperatures reaching as low as –40°C at an altitude of 2000m.

In the northern hemisphere we find an expansion into lower latitudes of the 0°C isotherm, compared to temperature gradients derived from oxygen isotope measurements of continental vertebrates (Amiot et al., 2004) and leaf margin analysis (Wolfe and Upchurch, 1987). On the North slope of Alaska, at a palaeolatitude of ∼80–85° N, analysis of fossil leaves leads to a MAT of 5°C (Spicer and Parrish, 1990) and 2–8°C for the Campanian and Maastrichtian (Parrish and Spicer, 1988). Our ensemble predict a range in MAT at 80° N of –13 to –3°C with an average summer temperature of 9–18°C. These differences between northern high-latitude palaeotemperature proxies and GCM predictions are significant, i.e. greater than the measurement errors, and so are difficult to reconcile.

Evidence using similar physiognomic analysis of fossil floras in the southern hemi-

sphere provides a more satisfactory quantitative comparison. On the Antarctic Peninsula at 59–62° S, a MAT of 7–15°C was derived (Francis and Poole, 2002; Poole et al., 2005), compared to GCM prediction of between 8.3–12.5°C for 1–6×CO_2. In addition, annual temperatures of ∼12–15°C and 7–16°C (Kennedy et al., 2002; Kennedy, 2003) were derived on the South Island, New Zealand, compared to GCM predicted range of 8.3–13.2°C. This apparent improvement in high-latitude performance could be a consequence of the poor representation of these regions within the GCM, in particular within the land-sea mask and orography fields.

5.2 Thermal seasonality

Comparing the Maas4^{CON} experiment against PreInd, we find regions of increased thermal seasonality, particularly in the ice-free high latitudes. Generally, no significant increase in seasonality is observed in the continental interiors, as predicted by Sloan and Barron (1990). The heat capacity of the epicontinental seaways provides a source of winter warmth to the continental interiors, buffering the effect of continentality. Bush and Philander (1997) found a reduction in seasonality, other than in Northern Africa and the northern extent of South America (where the palaeopositions are more equatorial), the HadCM3L experiments fail to support this. As CO_2 levels rise, we observe a general global increase in the intensity of the thermal seasonal cycle except in the Proto-Arctic Ocean and surrounding region where rising CO_2 leads to a reduction in seasonality.

The inclusion of the TRIFFID dynamic vegetation model, Maas4^{VEG}, results in a warming of summer temperatures more so than winter temperatures. Most northern hemisphere and high-latitude southern hemisphere landmasses experience a summer temperature increase of between 2 and 5°C. Peak warming occurs during the onset of summer, with warming as high as 8°C. Over Antarctica this summer warming is more pronounced, with minimal warming the remainder of the year. The summer warming results in an increase in thermal seasonality in these regions. This opposes the findings of Haywood and Valdes (2006), who found that implementing TRIFFID

led to a decrease in thermal seasonality for the mid Pliocene. In these experiments the seasonality signal is "buffered" by the presence of high-latitude ice. In the ice-free Maastrichtian experiments the high latitudes experience significant thermal seasonality and are therefore more sensitive to the changes in land surface scheme.

5.3 Precipitation and the hydrological cycle

Comparing the Maas4^{CON} with the PreInd experiment, the average global precipitation increases by 18%, increasing particular over land areas with a 26% increase (from 1.97 to 2.48 mm/yr). This enhanced hydrological cycle occurs mostly as increases in convective rainfall during the summer months. The distribution of these enhancements, as shown within Fig. 5, reflects the palaeo-distribution of the continents in relation to the ITZC; in particular over northern Africa, which experiences heavy precipitation (in agreement with Bush and Philander (1997)). This increase appears to be driven by the differences between the PreInd and Maas1 experiments rather than by elevated atmospheric CO_2 levels, as we only observe a 5% increase between the Maas1 and Maas6 experiment (see Table 1). We observe regions in the Maas4^{CON} experiment that experience a reduction in seasonal precipitation. In the tropical regions of South-East Asia, South America and South Africa we find a pronounced dry season during the winter months.

Increasing levels of atmospheric CO_2 leads to a redistribution of precipitation, increasing levels occurring mostly in the northern high-latitudes and tropics. Summer monsoons are predicted in Brazil, East Africa and northern India. With the TRIFFID dynamic vegetation model, Maas4^{VEG}, we observe an increase of 4% in the global average and 9% in the average land precipitation. The geographical distribution of these changes is complex, but generally we observe increases in the low and high latitude ocean precipitation and low to mid latitude land precipitation.

5.4 Surface ocean temperature

The Maas1 experiment predicts a globally averaged sea-surface temperature (SST) increase of 4.9°C over the PreInd experiment. With a quadrupling of CO_2 this increases to a 7.8°C difference, a value higher than previous predictions. For the Late Cretaceous, Bush and Philander (1997) found an increase of ∼5°C, whilst Otto-Bliesner et al. (2002) found a 3–4°C increase.

Zonally averaged plots of SST values can be seen in Fig. 6. In the equatorial, mid-latitude and high-latitude regions we find SST, for the 1–6×CO_2 scenarios, to be 2.2–7.5, 3.4–10.9 and 0.2–9.7°C warmer than the pre-industrial. The spatial distribution of SST for the PreInd and Maas4^{CON} can be seen within Fig. 7. We observe temperatures within the equatorial region between 26 and 34°C in a distribution similar, but slightly higher in magnitude, to Otto-Bliesner et al. (2002). The heating of the low latitude surface waters is supported by a number of isotopic and molecular measurements of well-preserved samples. These include the alkenone derived SSTs from planktonic foraminifera (Pearson et al., 2001) as well as $\delta^{18}O$ measurements of metastable carbonates (Wilson and Opdyke, 1996), fossil fish teeth (Pucéat et al., 2007), Molluscs and Planktonic foraminifera (Cochran et al., 2003; Zakharov et al., 2006). In the northern high latitude oceans, discrepancies between model data and proxies are significant. Using the Tex_{86} palaeotemperature proxy, Jenkyns et al. (2004) derived a early Maastrichtian temperature of ∼15±1°C at ∼80° N, possibly representative of a summer planktonic bloom. Within the GCM ensemble we find maximum mean summer temperatures of ∼7°C and a MAT of ∼2°C within the Maas6 experiment. Similar to land surface temperatures in this region, these data-model mismatches are difficult to reconcile.

5.5 Surface ocean salinity

Figure 8 shows the geographical distribution of sea-surface salinity for the PreInd and Maas4^{CON}. We find a pattern of elevated sea salinities in the subtropics and mid-

latitudes. Very low salinity is observed within the enclosed Arctic Ocean. Particularly high levels of salinity occur along the western coast of Africa, the North Atlantic Tethys, and the western Tethys. The sea-surface salinity reaches levels as high as 44.5 psu in the 4×CO_2 experiment. This exceeds previously predicted highs of 38.5 in the Gulf of Mexico (Bush and Philander, 1997) 38 in the western Tethys (Otto-Bliesner et al., 2002), 37 between southwestern Eurasia and North Africa (Bush and Philander, 1997), and ∼38 on the western sides of ocean basins within the equatorial belt (Hay and DeConto, 1999). The modelled spatial distribution of sea surface salinity compares well with that of Hay and DeConto (1999); Otto-Bliesner et al. (2002). In agreement with Hay and DeConto (1999) we find greater extremes in salinity gradients, which supports their assertion of a greater role of regional salinity differences in driving ocean circulation. As we increase concentrations of atmospheric CO_2 we find increasing levels of sea-surface salinities rather than changes in geographical distribution. The regions of high salinity correspond well with the descending arms of the Hadley cell where the dry air would have caused evaporation to exceed precipitation.

5.6 Surface ocean currents and dynamics

Circulation through the Tethys Ocean occurs in a general gyre-type motion. Tropical easterly winds and westerly winds in the mid latitudes drive a clockwise gyre circulation within the North Atlantic and between North Africa and Eurasia. No dominant eastward or westward flow is observed. This does not agree with the findings of Bush and Philander (1997), who predicted a general westward flow that joined with the subtropical Pacific current to form a westward circumglobal current. Although Barron and Peterson (1989) failed to observe a prominent westward flow in the mid-cretaceous Tethys, gyre circulation was present, in a mode similar to our predictions. This led them to predict a general eastward flow through the Tethys. Bush and Philander (1997) suggested this was a result of limited spatial resolution in the ocean model and possibly through the use of a mid-Cretaceous continental configuration. A possible explanation to this discrepancy is that the reconstructed flow through the Tethys depends on how extensive

the Tethys is at the time represented by the reconstruction. In addition, the flow is sensitive to the GCM boundary conditions in particular the land sea mask and bathymetry, this in turn being a function of palaeogeographic reconstruction accuracy, GCM spatial resolution and the skill involved in creating the boundary conditions. Figure 9 shows a plot of the magnitudes and vectors of the near surface ocean current for the PreInd and Maas4^{CON} experiments.

The geographical distribution of the annual mean mixed-layer depth (MLD) is shown within Fig. 10. Comparing the Maas4^{CON} against the PreInd, we find similar patterns in the northern Pacific but subdued mixing in the North Atlantic, reflecting its limited northward extension. Peak mixing occurs at the same time of year in both cases, typically between February and March. In the southern hemisphere of Maas4^{CON} we find a slightly later onset of maximum mixing (September compared to July). The MLD also extends to greater depths during peak mixing. Otto-Bliesner et al. (2002) found mixing in a pattern similar to Maas4^{CON} (shown in Fig. 10) with peak wintertime mixing occurring around the northwest boundary of the North Pacific and in a region west of Australia and south of Africa and India.

In the reduced atmospheric CO_2 experiments (Maas1 and Maas2), cooler and denser high-latitude surface waters, in response to a generally more vigourous ocean circulation, drive an increase in the depth of the oceanic mixed layer. In the case of Maas1 we find a mixed layer depth as deep as 2 km off the coast of East Antarctica. As the atmospheric CO_2 increases (as in Maas4 and Maas6) an inverse response is predicted, decreasing the depth of the oceanic mixed layer.

6 Discussion and future directions

We have presented the results of a computer modelling study of the Maastrichtian climate system, investigating the roles of geography, changing atmospheric CO_2 levels and modelled vegetation treatment.

Our results are not fully supportive of an equable climate system as we find a general increase in thermal seasonality, particularly at the higher latitudes. The inclusion of a realistic vegetation model leads to further increases in seasonality, as does increasing levels atmospheric CO_2. Only in a small number of regions, whose palaeopositions are more equatorial, do we observe a decrease in seasonality. We observe a reduction in latitudinal temperature gradient, particularly at the high latitudes, although direct comparison between the modern and Maastrichtian is complicated by changes in the land-sea distribution. Polar-regions are significantly warmer than present, primarily due to the lack of year-round polar ice.

We find a climate sensitivity of 3.9°C for a quadrupling of atmospheric CO_2, which is similar to the previous predictions of 3.6°C (Barron and Washington, 1985), 5.5°C (Barron et al., 1993) and 4°C (Bush and Philander, 1997). We find a larger 5.9°C warming due to the differences between the pre-industrial and Maas1 experiments, although we cannot associate this with a single driving factor such as the changes in geography, due to additional changes in the boundary conditions.

Using a more realistic land-surface treatment, through the implementation of the TRIFFID dynamic vegetation model, we find a smaller increase in global near-surface air temperatures than previously predicted (0.2°C compared to the 2.3°C found in the $2\times CO_2$ Maastrichtian experiment of Otto-Bliesner and Upchurch (1997). Warming occurs mostly over the mid to high latitudes, with the northern hemisphere and southern hemisphere high-latitudes experiencing increased thermal seasonality. In agreement with Otto-Bliesner and Upchurch (1997) we find peak high-latitude warming occurring during the summer months. We also observe an increase in the low-mid latitude annual mean precipitation.

Considering Maastrichtian ocean dynamics, we observe a gyre-type circulation through the Tethys, although we acknowledge that the flow is sensitive to the extent of the Tethys and how this is represented within the GCM boundary conditions. Global distributions of the salinity demonstrate similarities to previous predictions (Otto-Bliesner et al., 2002) although in regions we exceed previously calculated salinity maxima.

Greater regional differences in salinity, suggest a larger role of salinity in the circulation of the ocean than the present day.

Comparison of low and high latitude palaeotemperature proxies with GCM predictions presents a mixed picture. In the mid to low and southern high latitude regions, the broad estimates of the MAT from terrestrial vegetation and SSTs from planktonic foraminifera, compare well with the temperature envelope derived from the GCM ensemble. In the northern high latitudes we find unsatisfactory comparison between palaeotemperature proxy and GCM ensemble predictions, HadCM3L predicts MATs that are comparatively too cold.

For a long time, palaeoclimate modellers have faced problems in replicating high-latitude polar warmth whilst maintaining tropical temperatures that are in-line with geological proxies (Barron et al., 1981; Barron and Washington, 1985; Sloan and Barron, 1990; Schmidt and Mysak, 1996; Herman and Spicer, 1997). A number of possible deficiencies in current GCMs have been identified, whose mechanisms may play a more important and significant role in the global heat budget of warm greenhouse climates. The poleward transport of heat by an enhanced hydrological cycle (Hay and DeConto, 1999; Ufnar et al., 2004) and increased tropical cyclones (Emanuel, 2001; Sriver and Huber, 2007) as well as the role played by Polar Stratospheric Clouds in high latitude warming (Sloan and Pollard, 1998; Peters and Sloan, 2000) may have considerable roles in warmer climates. As shown within Otto-Bliesner and Upchurch (1997) and this study, the accurate representation of vegetation could also contribute. In addition, the representation of boundary conditions within the GCM, such as arctic seaway connections and epicontinental seas, are also important factors. The same model inadequacies may also play a role in the model-data mismatches found in the Cretaceous continental interiors (Spicer et al., 2008). Our ensemble, members of which form part of the Spicer et al. (2008) study, predict thermal seasonalities that are similar to the present day, in terms of the magnitude of the temperature envelope and cool annual-mean temperatures. This is in disagreement with the predictions made using leaf physiognomy analysis which suggests a warmer mean annual temperature and a

significantly reduced seasonal temperature range.

Future work will use these and additional modelled climates to drive an ice-sheet model to investigate concepts of *Southern* high-latitude glaciation. Although no direct sedimentary evidence, such as tills and ice rafted detritus, is available to support Maastrichtian glaciation (Frakes and Francis, 1988; Price, 1999), the possibility of significant glaciation is supported by indirect oxygen isotope measurements (Barrera and Savin, 1999; Li et al., 2000) and inferentially through sea level reconstructions (Miller et al., 1999, 2003, 2005).

An example of a eustatic sea-level signature believed to have a glacial origin is located at the Campanian/Maastrichtian boundary. Miller et al. (1999, 2003) associated a reconstructed sea level lowering (which they believe to be eustatic) at the boundary to the δ^{18}O increase (indicative of cooling) in both benthic and low latitude planktic foraminifera of Barrera and Savin (1999). Miller et al. (1999) had suggested that this high-point in benthic δ^{18}O at ~71 Ma was a consequence of a decrease in bottom water temperature that was incompatible with an ice-free world. Using a minimum of 50% contribution from ice sheets, the δ^{18}O values equated to a 20–40 m fall in sea level. It was suggested that these ice sheets, which were driven and maintained by orbital configurations providing minimal insolation during the summer season, were restricted to the mountain regions of Antarctic and remained inland, not reaching the coast (Miller et al., 2005). In this way, coastal Antarctica and the surrounding waters remained warm, maintaining compatibility with the presence of terrestrial flora supportive of relative warmth (Francis and Poole, 2002; Poole et al., 2005).

We aim to investigate the possibility of southern high-latitude Maastrichtian glaciation using an ice-sheet model driven by the predicted climates described in this paper. Additional GCM experiments have been carried out with orbits favourable for southern hemisphere glaciation; these will be used to investigate the extremes of possible orbital induced glaciation. Further sensitivity experiments will explore the climatic response to the presence of seaway connections to the Arctic.

7 Conclusions

The ensemble approach has allowed the climatic effects of a number of sensitivities to be investigated. The main findings to come out of this study are as follows:

1. We find a global averaged warming of 5.9°C, going from pre-industrial to the $1\times CO_2$ Maastrichtian boundary conditions. It is not possible to associate this to a single driving factor, as the differences in the two experiments are numerous (geography, land-surface scheme, reduced solar constant). Quadrupling CO_2 levels leads to a further warming of 3.9°C. The implementation of the TRIFFID dynamic vegetation model, at $4\times CO_2$, results in an average 0.2°C landmass warming, occurring mostly during summer

2. Other than in the northern high latitudes, ensemble derived land-surface and sea-surface temperatures are generally in good agreement with climate proxies. In the northern high-latitudes, differences between palaeotemperature proxies and GCM predictions are difficult to reconcile, suggesting deficiencies in the model boundary conditions and/or model physics

3. The $4\times CO_2$ Maastrichtian control experiment exhibits a 26% greater mean land-surface precipitation than the pre-industrial. This is driven principally by the differences between the $1\times CO_2$ Maastrichtian and the pre-industrial runs rather than through increased CO_2 levels. The implementation of TRIFFID results in a further 9% increase

4. The $1\times CO_2$ Maastrichtian experiment predicts globally averaged sea surface temperatures 4.9°C warmer than the pre-industrial. A quadrupling of CO_2 leads to a further 2.9°C warming

5. We find a pattern of elevated sea-surface salinities in the subtropics and mid-latitudes. Although we predict higher peak values, the geographical distribution

is in good agreement with previous predictions (Hay and DeConto, 1999; Otto-Bliesner et al., 2002). Increasing levels of atmospheric CO_2 leads to increasing salinities rather than changes in the geographical distribution

6. We find a wind and geography driven gyre-type circulation in the central Tethys, although it is suggested that this is sensitive to the construction and GCM representation of the land-sea mask and bathymetry.

7. In the $4\times CO_2$ Maastrichtian experiment we find a mixed layer depth (MLD) in the mid-high latitudes that extends significantly deeper than the pre-industrial. Decreasing levels of atmospheric CO_2 drive a deepening of the MLD.

Acknowledgements. The authors acknowledge funding from the Natural Environment Research Council Antarctic Funding Initiative grant NE/C506399/1 entitled "Terminal Cretaceous climate change and biotic response in Antarctica". We thank the British Antarctic Survey and H.M.S. Endurance for support for Antarctic fieldwork, and the Transantarctic Association and Antarctic Science Bursary for additional funding. We thank other members of the project for discussion – J. Francis (PI), V. Thorn, J. Marshall, A. Crame, R. Raiswell, P. Frost, D. Pirrie.

References

Amiot, R., Lécuyer, C., Buffetaut, E., Fluteau, F., Legendre, S., and Martineau, F.: Latitudinal temperature gradient during the Cretaceous Upper Campanian-Middle Maastrichtian: $\delta^{18}O$ record of continental vertebrates, Earth and Planetary Science Letters, 226, 255–272, 2004. 984, 992

Barrera, E.: Global environmental changes preceding the Cretaceous-Tertiary boundary: Early-late Maastrichtian transition, Geology, 22, 877–880, 1994. 983

Barrera, E. and Savin, S. M.: Evolution of late Campanian-Maastrichtian marine climates and oceans, Geological society of America, Special paper 332, 245–278, 1999. 1000

Barrera, E., Huber, B. T., Savin, S. M., and Webb, P. N.: Antarctic marine temperatures: Late Campanian through early Holocene, Paleoceanography, 2, 21–47, 1987. 984

Barron, E.: A warm equable Cretaceous: the nature of the problem, Earth-Science Reviews, 19, 305–338, 1983. 983, 984, 985

Barron, E. and Peterson, W. H.: Model simulation of the Cretaceous ocean circulation, Science, 244, 684–686, 1989. 987, 996

Barron, E. and Peterson, W. H.: Mid-Cretaceous ocean circulation: results from model sensitivity studies, Paleoceanography, 5, 319–337, 1992. 987

Barron, E., Fawcett, P., Pollard, D., and Thompson, S.: Model simulations of Cretaceous climates: the role of geography and carbon dioxide, Philos. Trans. R. Soc., Biological Sciences 341, 307–316, 1993. 985, 986, 998

Barron, E. J. and Washington, W. M.: Cretaceous climate: A comparison of atmospheric simulations with the geologic record, Palaeogeography, Palaeoclimatology, Palaeoecology, 40, 103–133, 1982. 984, 986

Barron, E. J. and Washington, W. M.: Warm Cretaceous climates: High atmospheric CO_2 as a plausible mechanism, in: The carbon cycle and atmospheric CO_2 : Natural Variations, Archean To present (Geophys Monogr. 32) AGU, edited by Sundquist, E. and Broeker, W., 546–553, Washington DC, 1985. 984, 985, 986, 998, 999

Barron, E. J., Thompson, S. L., and Schneider, S. H.: An ice-free Cretaceous? Results from climate model simulations, Science, 212, 501–508, 1981. 984, 999

Beerling, D. J., Lomax, B., Royer, D. L., Upchurch Jr., G. R., and Kump, L.: An Atmospheric pCO_2 reconstruction across the Cretaceous-Tertiary boundary from leaf megafossils, PNAS, 99, 7836–7840, 2002. 983

Brown, B., Gaina, C., and Müller, D. R.: Circum-Antarctic palaeobathymetry: Illustrated examples from Cenozoic to recent times, Palaeogeography, Palaeoclimatology, Palaeoecology, 231, 158–168, 2006. 983

Bush, A. B. G. and Philander, S. G. H.: The late Cretaceous: Simulation with a coupled atmosphere-ocean general circulation model, Paleoceanography, 12, 495–516, 1997. 985, 986, 987, 991, 992, 993, 994, 995, 996, 998

Case, A., Martin, J. E., Chaney, D. S., Reguero, M., Marenssi, S., Santillana, S, M., and Woodburne, M.: The first Duck-billed Dinosaur (Family Hadrosauridae) from Antarctica, Journal of Vertebrate Paleontology, 20, 612–614, 2000. 983

Cochran, J. K., Landman, N. H., Turekian, K. K., Michard, A., and Schrag, D. P.: Paleoceanography of the Late Cretaceous (Maastrichtian) Western Interior Seaway of North America: evidence from Sr and O isotopes, Palaeogeography, Palaeoclimatology, Palaeoecology, 191,

45–64, 2003. 995

Cojan, I., Moreau, M.-G., and Stott, L.: Stable carbon isotope stratigraphy of the Paleogene pedogenic series of southern France as a basis for continental marine correlation:, Geology, 28, 259–262, 2000. 983

Cosgrove, B. A., Barron, E., and Pollard, D.: A simple interactive vegetation model coupled to the GENESIS GCM, Global and Planetary Change, 32, 253–278, 2002. 986

Cox, P. M.: Description of the "TRIFFID" Dynamic Global Vegetation Model, Hadley centre technical note 24, 2001. 989

Cox, P. M., Betts, R. A., Jones, C., Spall, S. A., and Totterdell, I.: Modelling Vegetation and the Carbon Cycle as Interactive Elements of the Climate System, Proceedings of the RMS Millenium Conference, 2001. 989

Crowley, T. J., Short, D. A., Mengel, J. G., and North, G. R.: Role of Seasonality in the Evolution of Climate during the Last 100 Million years, Science, 231, 579–584, 1986. 985

DeConto, R. M., Hay, W. H., Thompson, S. L., and Bergengren, J.: Late Cretaceous climate and vegetation interactions: Cold continental interior paradox, Geological Society of America, Special paper 332, 391–406, 1999. 987

Emanuel, K.: Contribution of tropical cyclones to meridional heat transport by the oceans, J. Geophys. Res., 106, 14 771–14 781, 2001. 999

Exon, N. F., Kennett, J., and Malone, M. J.: Proceedings of the Ocean Drilling Program, Initial Reports 189, http://www-odp.tamu.edu/publications/189_IR/189ir.htm, 2001. 983

Frakes, L. A.: Climates through geological time, Elsevier, Amsterdam, 1979. 983

Frakes, L. A. and Francis, J. E.: A guide to Phanerozoic climates from high latitude ice-rafting in the Cretaceous, Nature, 333, 547–549, 1988. 1000

Francis, J. E. and Poole, I.: Cretaceous and early Tertiary climates of Antarctica: evidence from fossil wood, Palaeogeography, Palaeoclimatology, Palaeoecology, 182, 47–64, 2002. 983, 984, 993, 1000

Gallagher, S. J., Wagstaff, B. E., Baird, J. G., Wallace, M. W., and Li, C. L.: Southern high latitude climate variability in the Late Cretaceous greenhouse world, Global and Planetary Change, 60, 351–364, 2008. 983

Gent, P. R. and McWilliams, J. C.: Isopycnal mixing in ocean circulation models, Journal of Physical Oceanography, 20, 150–155, 1990. 988

Ghosh, P., Ghosh, P., and Bhattacharya, S. K.: CO_2 levels in the Late Palaeozoic and Mesozoic atmosphere from soil carbonate and organic matter, Satpura basin, Central India, Palaeo-

geography, Palaeoclimatology, Palaeoecology, 170, 219–236, 2001. 983
Gladstone, R. M., Ross, I., Valdes, P. J., Abe-Ouchi, A., Braconnot, P., Brewer, S., Kageyama, M., Kitoh, A., Legrande, A., Marti, O., et al.: Mid-Holocene NAO: A PMIP2 model intercomparison, Geophys. Res. Lett., 32, doi:10.1029/2005GL023 596, 2005. 988
Gordon, C., Cooper, C., Senior, C. A., Banks, H., Gregory, J. M., Johns, T. C., Mitchell, J. F. B., and Wood, R. A.: The simulation of SST, sea ice extents and ocean heat transports in a version of the Hadley Centre coupled model without flux adjustments, Clim. Dynam., 16, 147–168, 2000. 988
Gradstein, F. M. and Ogg, J. G.: A Phanerozoic Time Scale. Episodes 19 (1–2), 3–5, 1996. 990
Gregory, J. M. and Mitchell, J. F. B.: The climate response to CO_2 of the Hadley Center coupled AOGCM with and without flux adjustments, Geophys. Res. Lett., 24, 1943–1946, 1997. 988
Hallam, A.: A review of Mesozoic climates, Journal of the Geological Society, 142, 433–445, 1985. 983
Hay, W. W. and DeConto, R, M.: Comparison of modern and Late Cretaceous meridional energy transport and oceanography, Geological Society of America, Special paper 332, 283–299, 1999. 987, 996, 999, 1002
Haywood, A. M. and Valdes, P. J.: Modelling Pliocene warmth: contribution of atmosphere, oceans and cryosphere, Earth and Planetary Science Letters, 218, 363–377, 2004. 989
Haywood, A. M. and Valdes, P. J.: Vegetation cover in a warmer world simulated using a dynamic global vegetation model for the Mid-Pliocene, Palaeogeography, Palaeoclimatology, Palaeoecology, 237, 412–427, 2006. 993
Herman, A. B. and Spicer, R. A.: New quantitative palaeoclimate data for the Late Cretaceous Arctic: evidence for a warm polar ocean, Palaeogeography, Palaeoclimatology, Palaeoecology, 227–251, 1997. 999
Huber, B. T., Norris, R. D., and MacLeod, K. G.: Deep-sea paleotemperature record of extreme warmth during the Cretaceous, Geology, 30, 123–126, 2002. 984
Jenkyns, H. C., Forster, A., Schouten, S., and Sinninghe Damste, J. S.: High temperatures in the Late Cretaceous Arctic Ocean, Nature, 432, 888–892, 2004. 983, 995
Kennedy, E. M.: Late Cretaceous and Paleocene terrestrial climates of New Zealand: leaf fossil evidence from South Island assemblages, New Zealand Journal of Geology and Geophysics, 46, 295–306, 2003. 993
Kennedy, E. M., Spicer, R. A., and Rees, P. M.: Quantitative palaeoclimate estimates from Late

Cretaceous and Paleocene leaf floras in the northwest of the South Island, New Zealand, Palaeogeography, Palaeoclimatology, Palaeoecology, 184, 321–345, 2002. 984, 993
Kump, L., Kasting, J. F., and Crane, R. H.: The Earth System, Prentice Hall, New Jersey, 1999. 990
Lawver, L. A., Gahagan, L. M., and Coffin, M. F.: The development of paleoseaways around Antarctica, in: The Antarctic Paleoenvironment: A Perspective on Global Change Antarctic Research Series, edited by: Kennett, J. P. and Warnke, D. A., 56, 7–30, 1992. 983
Li, L. and Keller, G.: Maastrichtian climate, productivity and faunal turnovers in planktic foraminifera in South Atlantic DSDP sites 525A and 21, Marine Micropaleontology, 33, 55–86, 1998. 983
Li, L. and Keller, G.: Variability in Late Cretaceous climate and deep waters: evidence from stable isotopes, Marine Geology, 161, 171–190, 1999. 983
Li, L., Keller, G., Adatte, T., and Stinnesbeck, W.: Late Cretaceous sea-level changes in Tunisia: a multi-disciplinary approach, Journal of the Geological Society, 157, 447–458, 2000. 1000
Lunt, D. J., Ross, I., Hopley, P. J., and Valdes, P. J.: Modelling Late Oligocene C_4 grasses and climate, Palaeogeography, Palaeoclimatology, Palaeoecology, 251, 239–253, 2007. 989
Markwick, P. J. and Valdes, P. J.: Palaeo-digital elevation models for use as boundary conditions in coupled ocean-atmosphere GCM experiments: a Maastrichtian (late Cretaceous) example, Palaeogeography, Palaeoclimatology, Palaeoecology, 213, 37–63, 2004. 983, 990, 1010
Miller, K., Sugarman, P., Browning, J. V., Kominz, M. A., Hernández, J. C., Olsson, R. K., Wright, J. D., Feigenson, M. D., and Van Sickel, W.: Late Cretaceous chronology of large, rapid sea-level changes: Glacioeustasy during the greenhouse world, Geology, 31, 585–588, 2003. 1000
Miller, K. G., Olsson, R. K., Barrera, E., Sugarman, P. J., and Savin, S. M.: Does ice drive early Maastrichtian eustasy?, Geology, 27, 783–786, 1999. 1000
Miller, K. G., Wright, J. D., and Browning, J. V.: Visions of ice sheets in a greenhouse world, Marine Geology, 217, 215–231, 2005. 1000
Nordt, L., Atchley, S., and Dworkin, S.: Paleosol barometer indicates extreme fluctuations in atmospheric CO_2 across the Cretaceous-Tertiary boundary, Geology, 30, 703–706, 2002. 983
Nordt, L., Atchley, S., and Dworkin, S.: Terrestrial Evidence for Two Greenhouse Events in the Latest Cretaceous, GSA Today, 13, 4–9, 2003. 983

Otto-Bliesner, B. L. and Upchurch, Jr, G. R.: Vegetation-induced warming of high latitude regions during the Late Cretaceous period, Nature, 385, 804–807, 1997. 986, 992, 998, 999
Otto-Bliesner, B. L., Brady, E. C., and Shields, C.: Late Cretaceous ocean: Coupled simulations with the National Centre for Atmospheric Climate System Model, J. Geophys. Res., 107, 1–13, 2002. 987, 995, 996, 997, 998, 1002
Parrish, J. T. and Spicer, R. A.: Late Cretaceous terrestrial vegetation: A near -polar temperature curve, Geology, 16, 22–25, 1988. 984, 992
Pearson, P. N., Ditchfield, P. W., Singano, J., Harcourt-Brown, K. G., Nicholas, C. J., Olsson, R. K., Shackleton, N. J., and Hall, M. A.: Warm tropical sea surface temperatures in the Late Cretaceous and Eocene epochs, Nature, 413, 481–487, 2001. 983, 995
Peters, R. B. and Sloan, C. L.: High concentrations of greenhouse gases and polar stratospheric clouds: A possible solution to high-latitude faunal migration at the latest Paleocene thermal maximum, Geology, 28, 979–982, 2000. 999
Poole, I., Cantrill, D., and Utescher, T.: A multi-proxy approach to determine Antarctic terrestrial palaeoclimate during the Late Cretaceous and Early Tertiary, Palaeogeography, Palaeoclimatology, Palaeoecology, 222, 95–121, 2005. 984, 993, 1000
Price, G. D.: The evidence and implications of polar ice during the Mesozoic, Earth-Science Reviews, 48, 183–210, 1999. 1000
Pucéat, E., Lécuyer, C., Donnadieu, Y., Naveau, P., Cappetta, H., Ramstein, G., Huber, B. T., and Kriwet, J.: Fish tooth δ^{18}O revising Late Cretaceous meridional upper ocean water temperature gradients, Geological society of America, 35, 107–110, 2007. 995
Schmidt, G. A. and Mysak, L. A.: Can increased poleward heat transport explain the warm Cretaceous climate?, Paleoceanography, 11, 579–593, 1996. 999
Sloan, L. C. and Barron, E.: “Equable” climates during Earth history?, Geology, 18, 489–492, 1990. 983, 984, 985, 986, 993, 999
Sloan, L. C. and Pollard, D.: Polar strospheric clouds: A high latitude warming mechanism in an ancient greenhouse world, Geophys. Res. Lett., 25, 3517–3520, 1998. 999
Spicer, R. A. and Parrish, J. T.: Late Cretaceous-early Tertiary palaeoclimates of the northern high-latitudes: a quantative view, J. Geol. Soc. London, 147, 329–341, 1990. 992
Spicer, R. A., Ahlberg, A., Herman, A. B., Hofmann, C.-C., Raikevich, M., Valdes, P. J., and Markwick, P. J.: The Late Cretaceous continental interior of Siberia: A challenge for climate models, Earth and Planetary Science Letters, 267, 228–235, 2008. 999
Sriver, R. L. and Huber, M.: Observational evidence for an ocean heat pump induced by tropical

cyclones, Nature, 447, 577–580, 2007. 999
Ufnar, D. F., González, L. A., Ludvigson, G. A., Brenner, R. L., and Witzke, B. J.: Evidence for increased latent heat transport during the Cretaceous (Albian) greenhouse warming, Geological Society of America, 32, 1049–1052, 2004. 999
Upchurch, G. R., Otto-Bliesner, B. L., and Scotese, C.: Vegetation-Atmosphere Interactions and Their Role in Global Warming during the Latest Cretaceous, Philosophical Transactions: Biological Sciences,, 353, 97–112, 1998. 987
Valdes, P. J., Sellwood, B. W., and Price, D. A.: Evaluating Concepts of Cretaceous Equability, Palaeoclimates, 2, 139–158, 1996. 983
Wilson, P. A. and Opdyke, B. N.: Equatorial sea-surface temperatures for the Maastrichtian revealed through remarkable preservation of metastable carbonate, Geology, 24, 555–558, 1996. 995
Wolfe, J. A. and Upchurch, Jr, G. R.: North American nonmarine climates and vegetation during the Late Cretaceous, Palaeogeography, Palaeoclimatology, Palaeoecology, 61, 33–77, 1987. 983, 992
Zakharov, Y. D., Popov, A. M., Shigeta, Y., Smyshlyaeva, O. P., Sokolova, E. A., Nagendra, R., Velivetskaya, T. A., and Afanasyeva, T. B.: New Maastrichtian oxygen and carbon isotope record: Additional evidence for warm low latitudes, Geosciences Journal, 10, 347–367, 2006. 995

Table 1. Details of the GCM experiments conducted. The Maastrichtian experiments are a continuation of an initial 100 yr run with Maas4 boundary conditions; this is included within the indicated total run length. The superscripts indicate the $4\times CO_2$ control run (CON) and the TRIFFID dynamic vegetation model (VEG).

Experiment	Run Length	Averaging period	Atmospheric CO_2 (× pre-industrial)	MAT (°C)	Mean Annual Precipitation (mm/day)
Maas1	423	30	1	18.1	3.21
Maas2	200	30	2	20.4	3.32
$Maas4^{CON}$	200	30	4	22.0	3.33
Maas6	200	30	6	23.6	3.37
$Maas4^{VEG}$	200	30	4	22.2	3.47
PreInd	100	30	1	12.2	2.82

1009

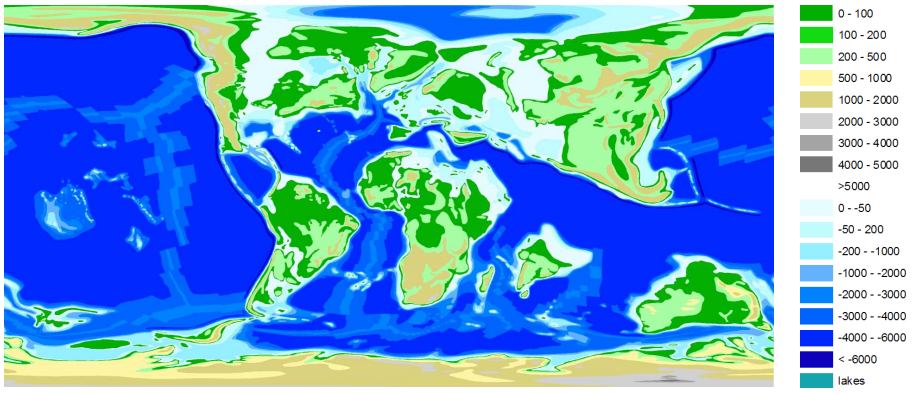

Fig. 1. The reconstruction of the Maastrichtian palaeogeography (heights in m) used within this study. Details of the reconstruction methodology can be found within Markwick and Valdes (2004).

1010

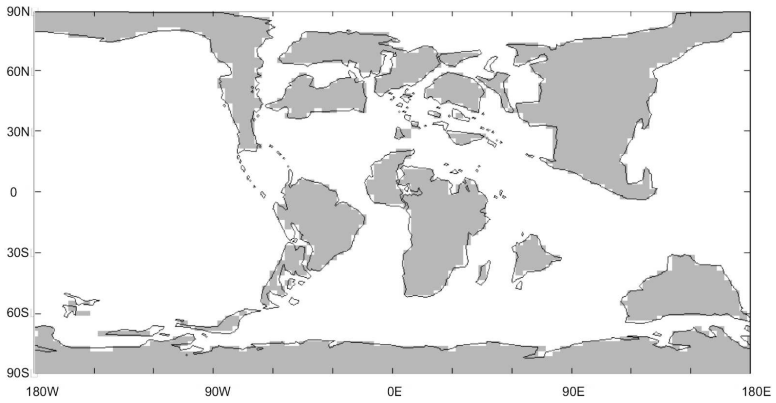

Fig. 2. The GCM land-sea mask.

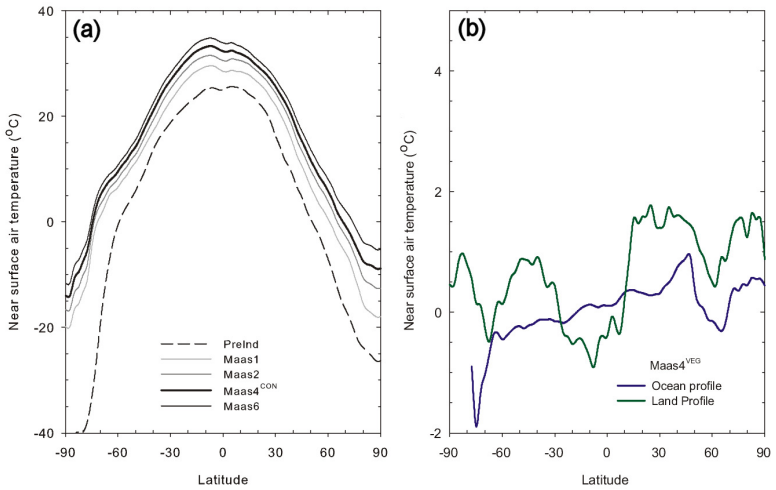

Fig. 3. **(a)** Global average plot of the meridional all-surface annual mean temperature distributions for the PreInd and 1–6×CO_2 Maastrichtian experiments. **(b)** Ocean and land surface plots of the differences between the Maas4^{CON} and the vegetation treatment, Maas4^{VEG}.

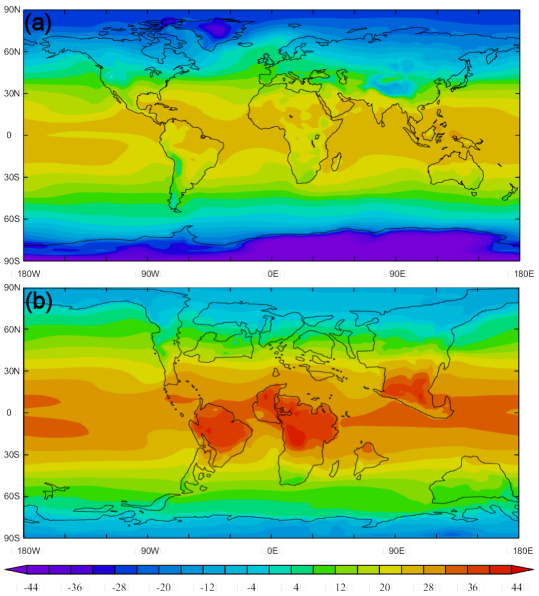

Fig. 4. Distribution of Mean annual surface air temperature for the **(a)** PreInd and the **(b)** Maas4^{CON} experiment.

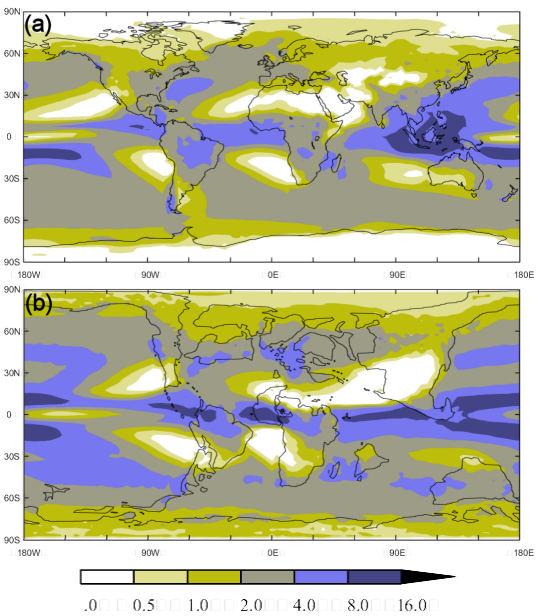

Fig. 5. Plots of annual mean precipitation (mm/day) in the **(a)** PreInd and **(b)** Maas4^{CON} experiment.

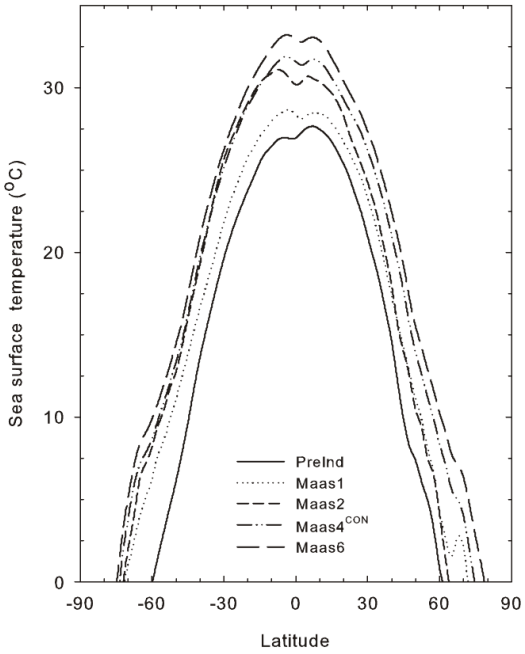

Fig. 6. Plot of the latitudinal annual mean SST distribution for PreInd and 1–6×CO_2 Maastrichtian experiments.

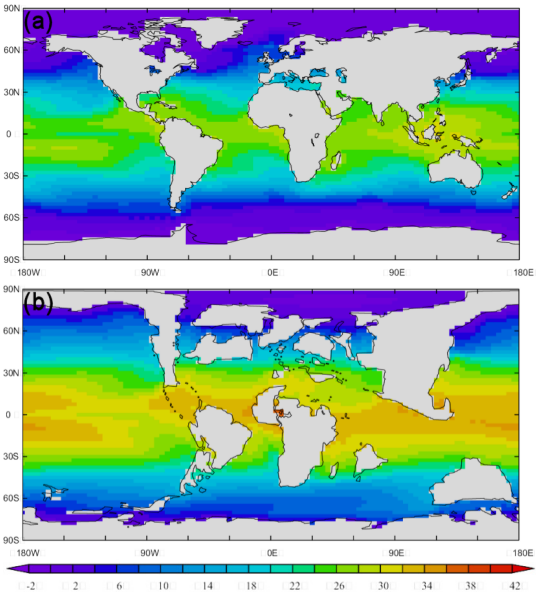

Fig. 7. Plots of the Sea Surface Temperature (°C) for the **(a)** PreInd and **(b)** Maas4^{CON}.

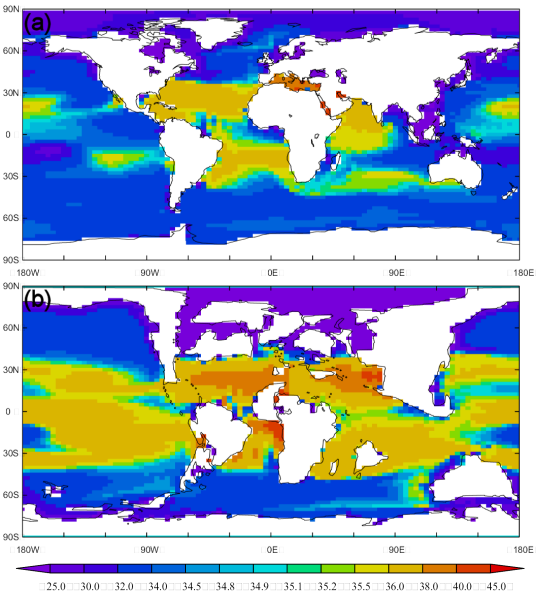

Fig. 8. Plots of the Sea Surface Salinity (psu) for the **(a)** PreInd and **(b)** Maas4^{CON}.

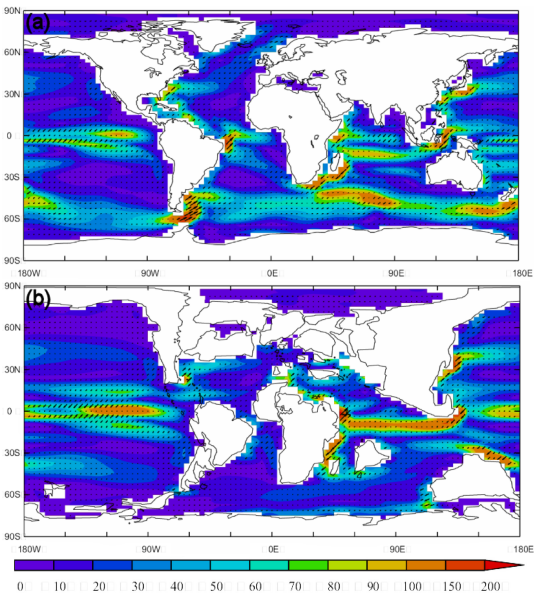

Fig. 9. Vector and magnitude plots of the mean annual upper-ocean currents for **(a)** PreInd and **(b)** Maas4^{CON}. The plots correspond to a GCM depth of between 67 and 78.5 m to avoid the wind driven Eckman component at the surface.

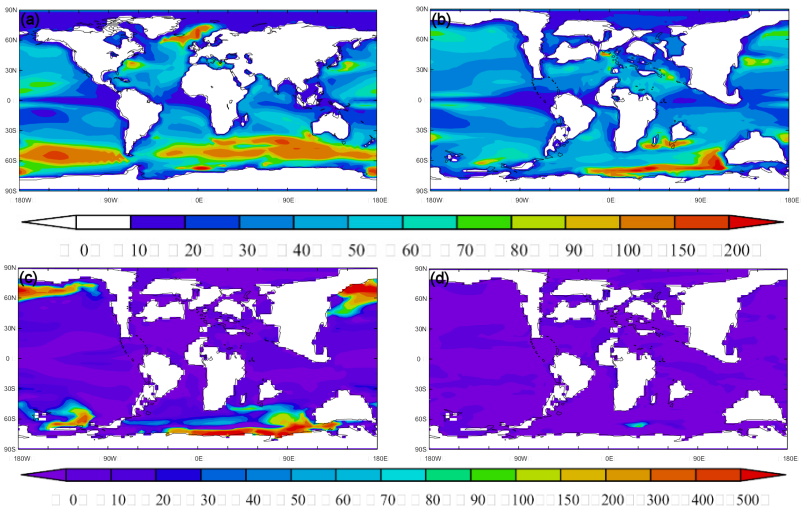

Fig. 10. Mixed layer depth for **(a)** PreInd, **(b)** Maas4^{CON} and the differences between Maas4^{CON} and the **(c)** Maas1 and **(d)** Maas6 experiments (e.g. Maas1-Maas4^{CON} so that red is indicative of greater depth than Maas4^{CON}).